

## Highlights

### **Markov property of the Super-MAG Auroral Electrojet Indices**

Simone Benella, Giuseppe Consolini, Mirko Stumpo, Tommaso Alberti, Jesper W. Gjerloev

- The SME index dynamics exhibits a complex behaviour and its statistics satisfy the Markov property for scales  $\lesssim 60$  min.
- The small scale dynamics is more complex than a diffusive process in time. A representation in terms of diffusion-jump process is discussed.
- The non-Markovian nature of the SME statistics for scales  $\gtrsim 60$  min is related to the metastability of the Earth's magnetospheric dynamics.

# Markov property of the Super-MAG Auroral Electrojet Indices

Simone Benella<sup>a</sup>, Giuseppe Consolini<sup>a</sup>, Mirko Stumpo<sup>b,a</sup>, Tommaso Alberti<sup>a</sup>, Jesper W. Gjerloev<sup>c</sup>

<sup>a</sup>*INAF-Istituto di Astrofisica e Planetologia Spaziali, INAF - Institute for Space Astrophysics and Planetology, Rome, 00133, Italy*

<sup>b</sup>*Department of Physics, University of Rome Tor Vergata, Via della Ricerca Scientifica, 1, Rome, 00133, Italy*

<sup>c</sup>*Johns Hopkins University, Applied Physics Laboratory, Laurel, 20723, MD, USA*

---

## Abstract

The dynamics of the Earth's magnetosphere presents dynamical complexity during magnetospheric substorms and geomagnetic storms. This complex dynamics comprises both stochastic and deterministic features occurring at different timescales. Here we investigate the stochastic nature of the magnetospheric substorm dynamics by analysing the Markovian character of the SuperMAG SME geomagnetic index, used as a proxy of the magnetospheric dynamics during magnetospheric substorms. In detail, performing the Chapman-Kolmogorov test, the SME dynamics appears to satisfy the Markov condition at scales below 200 minutes. The Kramer-Moyal analysis instead highlights that a purely diffusive process is not representative of the magnetospheric dynamics. Thus, a model comprising both diffusion and Poisson-jump processes is used to reproduce the SME dynamical features at small scales. A discussion of the similarities and differences between this model and the actual SME properties is provided with a special emphasis on the metastability of the Earth's magnetospheric dynamics. Finally, the relevance of our results in the framework of Space Weather is also addressed.

*Keywords:* Near-earth electromagnetic environment dynamics, Geomagnetic indices, Markov processes, Complex timeseries analysis

*PACS:* 0000, 1111

*2000 MSC:* 0000, 1111

---

## 1. Introduction

The near-Earth electromagnetic environment belongs to the class of far-from-equilibrium complex systems. Indeed, since early 90s it was realized that the Earth's magnetosphere response to solar wind changes at short timescales displays chaotic and nonlinear features [1, 2] that cannot be simply described in terms of an input-output linear system [3]. In the last two decades a clear evidence supporting the complex dynamics of the near-Earth electromagnetic environment has been provided in terms of hierarchical self-organized structures and criticality over a very wide range of timescales [3, 4, 5, 6, 7].

The dynamics of the geospace plasma environment is mainly controlled by the changes of the physical conditions of the interplanetary medium, i.e., the solar wind and the interplanetary magnetic field. These changes, driven by the solar activity, affect current systems flowing in the magnetosphere and ionosphere, in terms of both intensity and topology, as well as, produce an increase of the plasma transfer from the interplanetary medium to the Earth's magnetospheric cavity and the plasma convection inside the magnetosphere [8, 9, 10, 11]. The main manifestation of this interaction between the solar wind and the Earth's magnetosphere is the occurrence of magnetospheric substorms and geomagnetic storms.

The response of the geospace plasma environment to the interplanetary medium changes and the dynamics of the magnetosphere-ionosphere system can be monitored by using different geomagnetic indices, mainly derived from the temporal variations of ground-based magnetic field records from geomagnetic observatories. In detail, some of these indices, such as the Auroral Electrojet (AE) and  $D_{st}$ -type indices, are proxies of the dynamics of the currents flowing in the magnetosphere-ionosphere system [12, 13]. Among these geomagnetic indices the AE-indices, which are related to the occurrence of magnetospheric substorms, provides one of the most relevant proxies to investigate the magnetospheric dynamics with a special emphasis to the dynamics of the Earth's magnetospheric central plasma sheet (CPS). Indeed, the dynamics of the plasma in the near-Earth CPS is strictly related to the currents flowing in the auroral regions (the auroral electrojets) of which AE-indices are proxies. However, although AE-indices are one of the best proxies for the substorm dynamics, they still present some limitations in correctly estimating the auroral electrojet current intensity in the case of strong geomagnetic activity, when the auroral oval expands to lower

latitudes. Nowadays, to attempt to overcome these limitations an extended version of high-latitude indices, SME, SML and SMU, based on a large number (about 300) of currently operating ground-based geomagnetic observatories has been introduced by the SuperMAG collaboration [14]. This new set of indices seems to be capable of better monitoring the magnetospheric dynamics during substorms.

Since their introduction, the AE indices have been extensively used as a proxy of the global magnetospheric dynamics and, in particular, to model the magnetospheric dynamics during substorms [15, 16, 17, 18, 19, 20]. In detail, using AE-index as a descriptor of magnetospheric response to interplanetary medium changes, Pulkkinen et al. [17] showed that the Langevin dynamics is quite satisfactory in reproducing the main statistical features of the dynamics in the frequency range  $[0.07, 3]$  mHz. They indeed found the evidence that the AE Probability distribution function (PDF) can be estimated by solving the stationary Fokker-Planck (FP) equation and that the statistics of waiting times between subsequent bursts retrieved through their model is consistent with observations.

In the framework of complex time series analysis, the modeling of a variety of physical processes through FP equation frequently allows to capture important properties of the dynamics. In such cases, the processes satisfy the Markov condition and then the estimation of the first two Kramers-Moyal (KM) coefficients, i.e. the *drift* and *diffusion* terms, represents a fundamental starting point for both statistical analysis and modeling. This has been pointed out in many fields such as turbulence, economy, finance, neuroscience, cardiology, surface science and so forth [e.g., see 21, for a comprehensive review on this topic]. It is worth reminding that the FP is based on the assumption that the dynamics can be fully described by the first- and second-order KM coefficients as a simple drift-diffusion process and then all the KM coefficients of order  $\geq 3$  vanishes (see Section 3). However, such crucial requirement has never been verified in the case of AE index, or, more in general, for the magnetospheric dynamics in response to solar wind changes. Moreover, moving to frequencies below 0.07 mHz, many of the aforementioned models lose their validity since the history of the AE index starts affecting the magnetospheric dynamics in a non-trivial way, being the transfer of information not local in time as required by the Markov property.

The aim of this work is to apply the general analysis of Markov property and KM coefficients in the case of the magnetospheric dynamics in order to characterize its properties over a wide range of time scales. To this target in

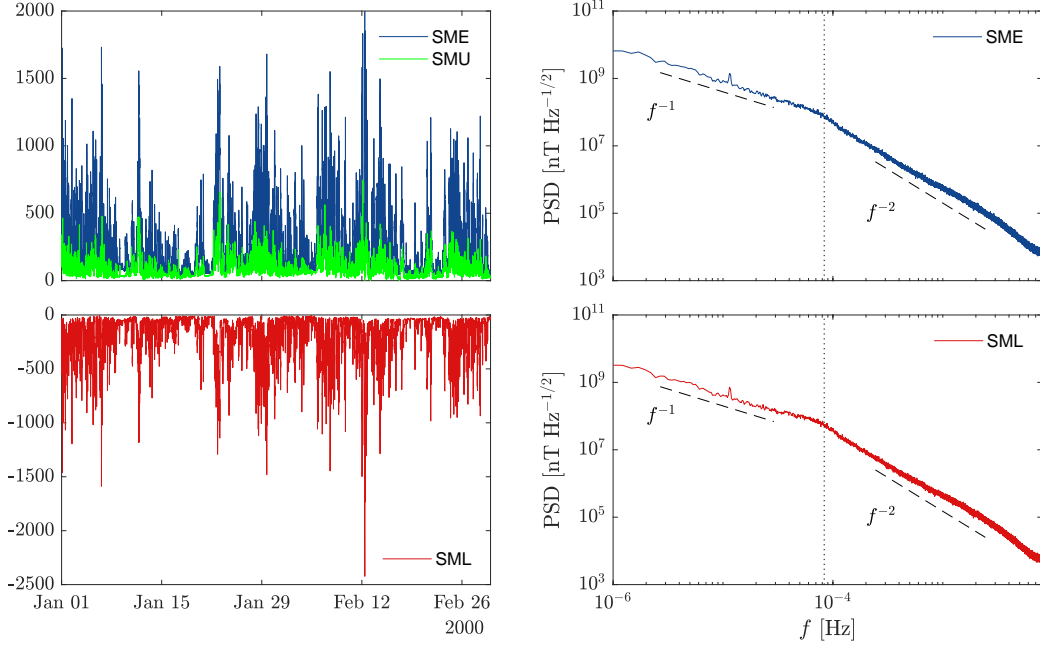


Figure 1: Left: A sketch of the SME (blue line), SMU (green line) and SML (red line) indices time series. Right: Power spectral density of the SME and SML indices. Dashed lines are a guide for the eye and represent the  $f^\beta$  with  $\beta = -1$  and  $\beta = -2$  spectral trends. The vertical dotted line denotes the spectral break located at  $\sim 8 \times 10^{-5}$  Hz.

our analysis instead of the AE-indices we use the SuperMAG indices, SME and SML.

Our work is organized as follows. A complete description of the data is presented in Section 2 and a summary of the methods involved in the analysis are provided in Section 3. the analysis presented in this work can be structured in two parts. The first is referred to the investigation of the Markov property for SME and SML dynamics, Section 4.1. The second part is devoted to the modeling of the SME index at small-scales and to study its Markov property as a function of the time scale, Section 4.2. Finally, discussion and conclusions are drawn in Section 5.

## 2. Data

In order to study the magnetospheric dynamics in response to interplanetary medium changes during geomagnetic substorms, in this work we use

the Super-MAG auroral electrojet indices SME and SML, which are a generalization of the traditional AE and AL indices, respectively [22]. These indices are indeed based on a larger set of ground-based magnetic field measurements coming from about 300 of geomagnetic observatories which extend to lower latitude in respect to the set of geomagnetic observatories used to compute AE-indices. This larger dataset allows to get a better estimation of the auroral electrojet current changes when the auroral oval extends to lower latitudes during strong geomagnetic substorms.

The analysis is carried out on SME and SML indices time series at 1-minute resolution ranging from 1995 to 2015 and thus covering the entire Solar cycle 23 and most of the cycle 24. Since these indices is rounded to integer nT values we added a uniform white noise with values  $\in [-0.5, 0.5]$  nT to the signal, in order to avoid issues due to the digitalization in the analysis. A sketch of SME and SML time series, along with their difference SMU, recorded between January and March 2000 are reported in the left column of Figure 1. The SME and SML power spectral densities are displayed in the right column of Figure 1. Exactly as for the case of the AE and AL indices, they appear as colored noises  $f^{-\beta}$  with two separate regimes: a  $\beta \sim -1$  region below  $\sim 0.08$  mHz and a  $\beta \sim -2$  region at higher frequencies. The spectral break of  $\sim 0.08$  mHz corresponds to  $\sim 200$  min and reflects some fundamental properties of the magnetospheric dynamics [1, 23, 24, 25]. Indeed, temporal scales below 200 min have been associated with the occurrence of fast relaxation process occurring in the CPS of the magnetospheric tails, which are associated with the internal dynamics of the Earth's magnetosphere in response to interplanetary medium changes [26, 27, 6]. Here, we will discuss and characterize this dynamical transition in terms of Markov processes.

### 3. Methods

By assuming that SME and SML time series can be assimilated to a generic stochastic process  $x(t)$ , the Markov property is, then, expressed in terms of the  $n$ -points transition probability

$$p[x_n, t + n\tau | x_{n-1}, t + (n-1)\tau; \dots; x_0, t] = p[x_n, t + n\tau | x_{n-1}, t + (n-1)\tau], \quad (1)$$

where the transition probabilities can be defined through the Bayes' formula as

$$p(x_1, t + \tau | x_0, t) = \frac{p(x_1, t + \tau; x_0, t)}{p(x_0, t)}. \quad (2)$$

Equations (1) and (2) tell us the main property of a Markov process, i.e. the knowledge of the initial distribution  $p(x_0, t)$  and the transition probabilities allows to define the complete  $n$ -point probability distribution of the considered process. This can also be expressed, for a Markov process, by the Chapman-Kolmogorov (CK) equation which reads as

$$p(x_2, t + 2\tau | x_0, t) = \int_{-\infty}^{+\infty} p(x_2, t + 2\tau | x_1, t + \tau) p(x_1, t + \tau | x_0, t) dx_1. \quad (3)$$

The differential form of Equation (3) expresses the time evolution of the transition probability and it is called the *master equation*, here reported in terms of the well-known Kramers-Moyal (KM) expansion

$$\frac{\partial}{\partial t} p(x_1, t + \tau | x_0, t) = \mathcal{L}_{KM}(x) p(x_1, t + \tau | x_0, t), \quad (4)$$

where  $\mathcal{L}_{KM}(x)$  is the KM operator

$$\mathcal{L}_{KM}(x) = \sum_{k=1}^{\infty} \left( -\frac{\partial}{\partial x} \right)^k D^{(k)}(x). \quad (5)$$

The functions  $D^{(k)}(x)$  are called KM coefficients and are defined as

$$D^{(k)}(x) = \frac{1}{k!} \lim_{\tau \rightarrow 0} \frac{M^{(k)}(x, \tau)}{\tau}, \quad (6)$$

where  $M^{(k)}$  are the conditional moments

$$M^{(k)}(x, \tau) = \int_{-\infty}^{+\infty} (x' - x)^k p(x', t + \tau | x, t) dx'. \quad (7)$$

As can be easily realized, the KM coefficients are not directly accessible from experimental timeseries, but rather one can compute the conditional moments at the data time resolution. Thus, one can approximate the KM coefficients as their “finite-scale” version evaluated for  $\Delta\tau$  equals to the data time resolution  $\tau_s$

$$D_{\tau_s}^{(k)}(x) = \frac{1}{k! \tau_s} M^{(k)}(x, \tau_s). \quad (8)$$

Equation (4) contains an infinite series of KM coefficients. The Pawula's theorem states that  $D^{(k)} = 0$  for  $k \geq 3$  if the fourth-order coefficient vanishes. In such case, the KM expansion reduces to the Fokker-Planck equation [28].

Empirical time series may exhibit fluctuations interrupted by sudden jumps between different states of the system, occurring in a very short time. However, such pronounced discontinuities can be introduced by the finite sampling of the underlying process that in principle can be or not a continuous diffusion process in the  $\tau_s \rightarrow 0$  limit. For a pure, statistically continuous, diffusive process, the state of the system as a function of time is described by the well-known Langevin equation

$$dx_t = a(x)dt + b(x)dW_t, \quad (9)$$

where  $a(x) = D^{(1)}(x)$  is the *drift* term and  $b(x) = \sqrt{2D^{(2)}(x)}$  modulates the *diffusion* term represented by the Wiener process  $W_t$ . However, the finiteness of the sampling time  $\tau_s$  can introduce spurious effects in the *finite-time* KM coefficient estimation such as non-vanishing high-order coefficients. A test for the Pawula's theorem, enabling to state whether or not the process can be considered as a continuous diffusion, was introduced by Lehnertz et al. [29]. In detail, for a general Langevin process, thus also including the case of multiplicative noise, exists the following linear relation between second- and fourth-order conditional moments for small values of  $\tau$ :

$$M^{(4)}(x, \tau) \simeq 3[M^{(2)}(x, \tau)]^2. \quad (10)$$

The above relation can thus be used as a test of validity of the Pawula's theorem by inspecting only conditional moments, that are directly accessible from data. In the following we will show that in the case of the SME and SML indices the simple Langevin model (9) does not represent an accurate description of the observed dynamics. This fact implies the existence of non-vanishing high-order KM coefficients that can be related to jump processes as we will show in the following.



## 4. Results

### 4.1. Analysis of the Markov property of SME and SML indices

We start our analysis of Markov features of SME and SML by checking the validity of the CK equation at different timescales [21]. Let us refer to the left-hand side of Equation (3) as *empirical probability*,  $p_E$ , and to the right-hand side as *CK probability*,  $p_{CK}$ . Equation (3) states that  $p_E = p_{CK}$  and the validity of such relation for the considered dataset provides information about the validity of the Markov property. We performed the CK test over different time scales and we report here three cases:  $\tau = 10$  min,  $\tau = 60$  min and  $\tau = 200$  min. If we define the process  $x_0(t) = x(t)$  as the SME index time series, the intermediate-scale process involved in the CK equation is  $x_1(t, \tau) = x(t + \tau/2)$  and the large-scale process is defined as  $x_2(t, \tau) = x(t + \tau)$ . We remark that the even spaced time separations, i.e.,  $0, \tau/2, \tau$  considered here, are chosen for simplicity. The same results hold for any  $0 < \tau' < \tau$  (not shown).

The CK test results are reported in Figure 2. In particular, Figure 2a and 2b show the good agreement between the level curves obtained for  $p_E$  (blue) and  $p_{CK}$  (red). This is also highlighted by cutting PDFs at  $x_0 = 500$  nT (Figure 2d-2e). Hence, we argue that the SME index satisfies the Markov property at scales up to 60 min. Conversely, by looking at  $\tau = 200$  min (Figure 2c) we clearly observe a departure of the empirical distribution  $p_E$  from the CK prediction  $p_{CK}$ , also highlighted by cutting PDFs at  $x_0 = 500$  nT (Figure 2f). This finding suggests that at scales  $\tau \gtrsim 200$  min the Markov condition is lost for the SME index. Thus, the fast dynamics of the SME index (i.e., at timescales shorter than 60 min) exhibits a “memoryless” character, while non-localtime correlations become important for the slow dynamics (i.e.,  $\tau \gtrsim 200$  min). Similar results are also found for the SML index (not shown).

Since SME and SML indices appear to be Markovian over a wide range of scales we evaluate the first-, the second- and the fourth-order KM coefficients at the finite time scale  $\tau_s = 1$  min as a function of the index value (Figure 3). The interval for KM coefficients estimation considered here is limited to 1000 nT for both SME and  $-SML$ , since for larger values the statistics is not sufficient to estimate the coefficients correctly. First- and second-order KM coefficients, related to the *drift* and *diffusion* terms of the corresponding Langevin equation, show a dependence on the SME index values that is similar to that observed for the AE index [17], Figures 3a and 3b. The

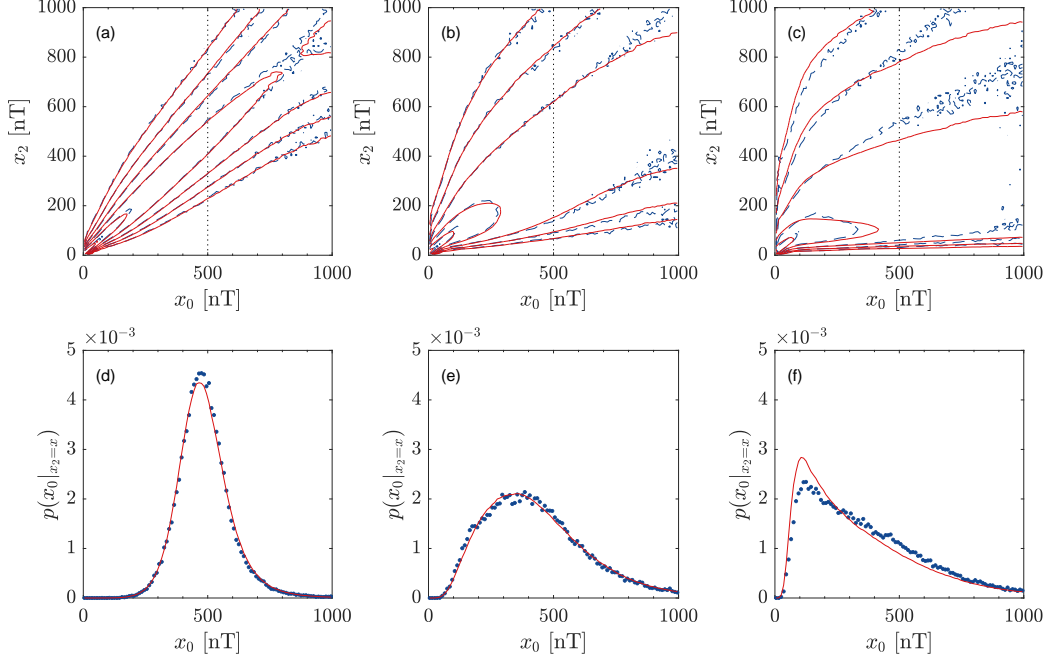


Figure 2: Results of the CK test of the SME index at different time scales. In the top panels is reported the comparison between  $p_E$  (blue) and  $p_{CK}$  (red) for different time scales: (a)  $\tau = 10$  min, (b)  $\tau = 60$  min and (c)  $\tau = 200$  min. In the bottom panels are reported PDFs obtained by cutting the corresponding  $p_E$  and  $p_{CK}$  at  $x_0 = 500$  nT for (d)  $\tau = 10$  min, (e)  $\tau = 60$  min and (f)  $\tau = 200$  min.

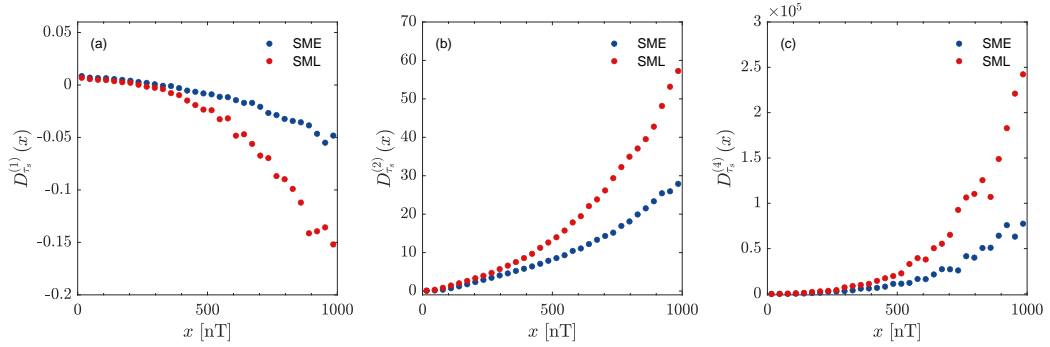


Figure 3: Finite-time KM coefficients  $D^{(1)}(x)$ ,  $D^{(2)}(x)$  and  $D^{(4)}(x)$  of the SME (blue) and  $-SML$  (red) indices time-series. The computation is performed with  $\tau = \tau_s = 1$  min.

same analysis, performed on the SML index, produces a similar trend of the KM coefficients although with different amplitudes. In particular, the deterministic term  $D_{\tau_s}^{(1)}(x)$ , associated with the drift, decreases more rapidly with respect to SME, whereas the stochastic term  $D_{\tau_s}^{(2)}(x)$  shows a faster increase. A similar trend is also observed for higher-order stochastic terms associated with  $D_{\tau_s}^{(4)}(x, \tau)$ , with both SME and SML indices having non-vanishing fourth-order KM coefficients (Figure 3c) that cannot be related to a finite-time effect. Indeed, by looking at the dependence of the moments  $M_{\tau_s}^{(4)}(x, \tau)$  on  $M_{\tau_s}^{(2)}(x, \tau)$ , Figure 4, a clear deviation from the expected theoretical linear behavior for a Langevin process (red line), as expected according to Equation (10), is observed. For sake of comparison, we also report the same relation for an Ornstein-Uhlenbeck process with  $D^{(1)}(x) = -x$  and  $D^{(2)}(x) = 1$ , showing an excellent agreement with is Equation (10). Hence, the non-vanishing high-order KM coefficients observed in this work constitute a physical feature of SME and SML index dynamics. Indeed, the larger drift coefficient of SME with respect to SML for increasing values of  $x$ , suggests that the deterministic component of SME is mainly related to magnetospheric convective processes, described via SMU (we remark that  $\text{SME} = \text{SMU} - \text{SML}$ ). Conversely, the larger values of high-order KM coefficients found for SML suggest that the major contribution to the stochastic terms of the SME dynamics can be ascribed to the burst-like activity of the geomagnetic tail.

#### 4.2. Diffusion-jump model for the SME index dynamics

As shown in the previous section, high-order KM coefficients are not vanishing for SME and SML indices. From a stochastic process perspective, this suggests that the magnetospheric dynamics cannot be represented as a continuous diffusion process, but it is characterized by jumps that are related to the observed bust-like activity. Henceforth we will focus on the SME index dynamics. Our purpose is to show that the SME index can be modeled as a stochastic process by adding a Poisson-like jump process to the Langevin dynamics as follows

$$dx_t = a(x)dt + b(x)dW_t + \xi dJ_t, \quad (11)$$

where  $a(x)$  is the drift term,  $b(x)$  is the diffusion strength of the Wiener process  $W_t$ , and  $\xi$  is the jump size of the Poisson jump process  $J_t$ . By assuming that the jump size  $\xi$  follows a Gaussian distribution, i.e.,  $\xi \sim$

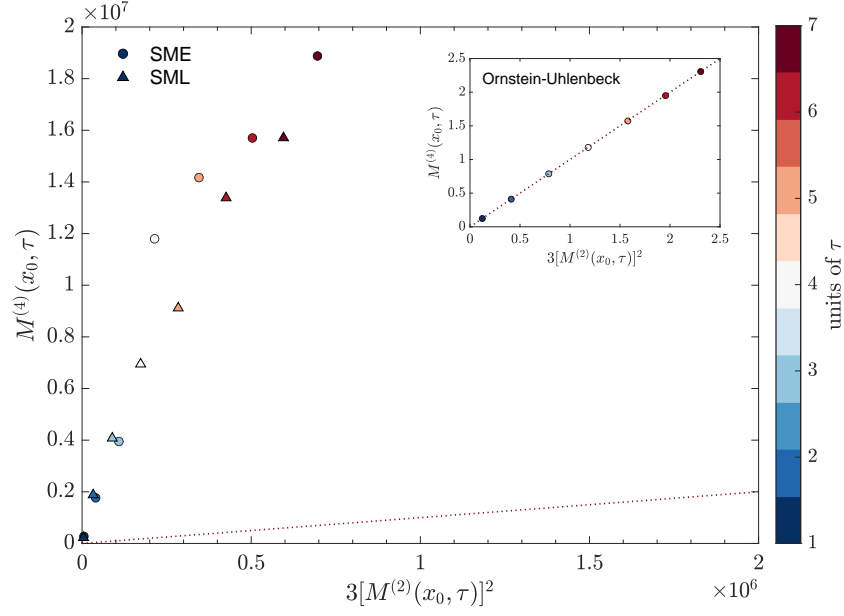


Figure 4: Scatter plot of the fourth-order moment  $M^{(4)}(x_0, \tau)$  vs  $3[M^{(2)}(x_0, \tau)]^2$  for SME (circles) and  $-SML$  (triangles) indices. The inset shows the same scatter-plot obtained in the case of the Ornstein-Uhlenbeck process. We chose  $x_0$  around the peak of the probability distribution functions, i.e.  $x_0 \sim 80$  nT for SME,  $x_0 \sim 50$  nT for  $-SML$  and  $x_0 \sim 0$  for the Ornstein-Uhlenbeck process. The colormap indicates the different values of  $\tau$  involved in the moment calculation in unit of time steps:  $\tau = 1$  min for SME/SML and  $\tau = 0.1$ , i.e. the integration time-step used for the Ornstein-Uhlenbeck process.

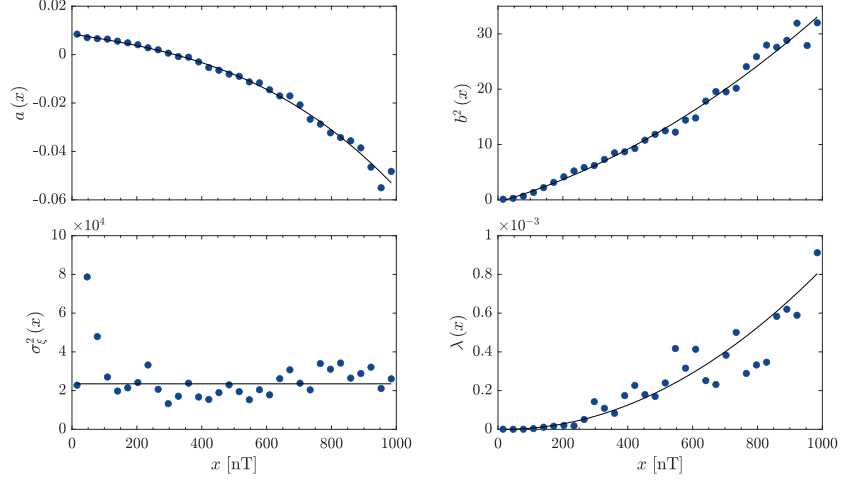


Figure 5: Diffusion-jump process parameters estimated from the high-order conditional moments of the SME time series. The parameters are the drift term  $a(x)$ , diffusion term  $b(x)$ , jump amplitude  $\sigma_\xi^2(x)$  and the jump rate  $\lambda(x)$ . Solid lines represent polynomial parameterizations.

$\mathcal{N}(0, \sigma_\xi)$ , the terms appearing in Equation (11) can be related to the KM coefficients [30]

$$\begin{aligned} a(x) &= D^{(1)}(x), \\ b^2(x) &= 2D^{(2)}(x) - \lambda(x)\sigma_\xi^2(x), \\ \lambda(x)[\sigma_\xi^2(x)]^n &= 2^n n! D^{(2n)}(x), \quad n > 2. \end{aligned} \tag{12}$$

By inverting Equation (12), we can estimate the jump size variance  $\sigma_\xi^2(x)$ , also called jump amplitude, and the jump rate  $\lambda(x)$  as

$$\sigma_\xi^2(x) = \frac{6D^{(6)}(x)}{D^{(4)}(x)}, \quad \lambda(x) = \frac{8D^{(4)}(x)}{\sigma_\xi^4}. \tag{13}$$

The derived parameters of the diffusion-jump from the high-order KM coefficients are reported in Figure 5. The typical burst-like activity of the magnetospheric dynamics, joined with the lowering of the statistics for higher values of the SME index, produces a noisy estimation of the high-order conditional moments, affecting the estimation of jump parameters, as observed in Figure 5. By using polynomial expansions as a function of the SME index values

(denoted by  $x$ ) we can provide an analytical form of the four parameters

$$\begin{aligned}
a(x) &= 0.0085 - 2.08 \times 10^{-5}x - 7.60 \times 10^{-9}x^2 - 3.53 \times 10^{-11}x^3, \\
b^2(x) &= -0.40 + 0.017x + 1.73 \times 10^{-5}x^2, \\
\sigma_\xi^2(x) &= 2.35 \times 10^4, \\
\lambda(x) &= -3.22 \times 10^{-8}x + 8.63 \times 10^{-10}x^2.
\end{aligned}$$

The drift  $a(x)$  and diffusion  $b^2(x)$  terms are in agreement with previous findings by Pulkkinen et al. [17] on the AE index, whereas the jump process appear to have a mean jump amplitude of  $\sim 2.35 \times 10^4$  nT<sup>2</sup> for any  $x$  and an occurrence rate increasing as the SME index values with a quadratic trend. The definition of the diffusion and jump processes allows us to integrate the Equation (11) by using a jump-adapted strong integration scheme for stochastic differential equation (SDE). Since the diffusion part is constituted by a multiplicative noise term, we adopt an integrator based on the Milstein scheme [31]

$$\begin{aligned}
x_{t_{n+1}-} &= x_{t_n} + a(x_{t_n})\Delta_{t_n} + b(x_{t_n})\Delta W_{t_n} + \\
&\quad \frac{b(x_{t_n})b'(x_{t_n})}{2}\{(\Delta W_{t_n})^2 - \Delta_{t_n}\}, \\
x_{t_{n+1}} &= x_{t_{n+1}-} + c(x_{t_{n+1}-})\{J_{t_{n+1}} - J_{t_{n+1}-}\}.
\end{aligned} \tag{14}$$

In Figure 6 we report a comparison between a portion of the SME index (top panel) and a realization of the SDE integration (middle panel). According to [17], the integration time step  $t_{n+1} - t_n$  is set equivalent to 5 s. The Wiener and Poisson processes obtained through the stochastic integration on this particular sample are reported in the bottom panel. From a visual inspection we observe as many features of the SME index time series are present also in the diffusion-jump process. In particular, middle and bottom panels show how the typical bursty character of the SME index can be well reproduced through the jump process. This is confirmed also by the comparison between the PDFs of the SME index and the diffusion-jump process, Figure 7. The comparison between the PDFs is shown in the interval  $[0, 1000]$  nT, which is the interval over which diffusion and jump parameters are estimated. However, good agreement between PDFs extends up to  $\sim 2000$  nT, after which the SME statistics shows a sudden increase related to extreme events, sometimes called *supersubstorms* [32], which are not reproduced by the SDE.

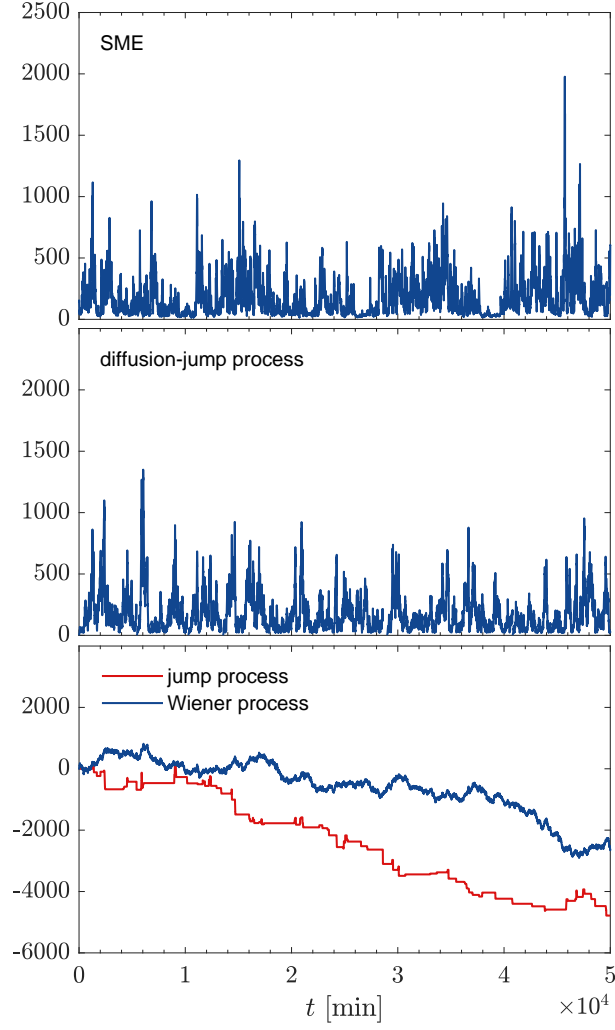


Figure 6: Top panel: sketch of  $10^4$  data points of the SME index time series. Middle panel: sketch of  $10^4$  data points obtained by integrating the SDE model of Equation (14) with the parameters of Figure 5. Bottom panel: diffusion and jump processes corresponding to the time series depicted in the middle panel.

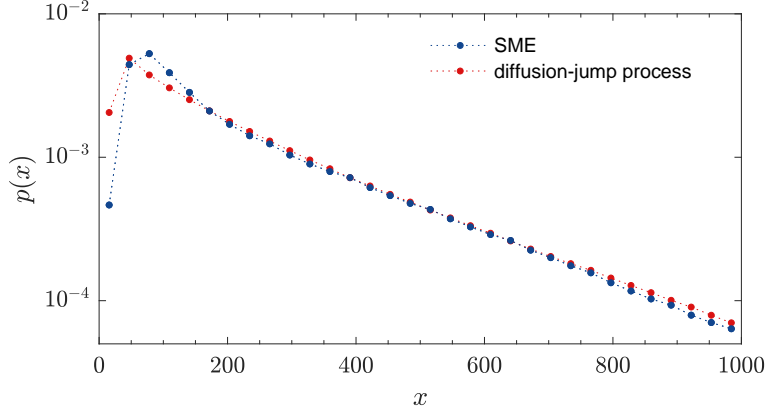


Figure 7: Comparison between the PDFs of the SME index (blue dots) and the SDE model (red dots).

As a final step, we emphasize the following remark. The CK test pointed out that the SME index statistics appears to violate the Markov property for time scales  $\tau \sim 60$  min (see Figure 2). On the contrary, the model defined by Equation (14) is Markovian at any scale as it is defined. Hence, it is natural to quantify the transition from a Markovian to a non-Markovian dynamics of the SME index by comparing its behavior to the one of a set of realizations of the model (Equation 14) as a function of the time scale. For this purpose, we introduce the Kullback-Leibler (KL) divergence as a functional enabling to quantify the goodness of the CK transition probability in approximating the empirical PDF as a function of the time scale  $\tau$

$$D_{KL}(p_E||p_{CK}) = \iint p_E(x_2, \tau_2; x_0, \tau_1) \log \frac{p_E(x_2, \tau_2; x_0, \tau_0)}{p_{CK}(x_2, \tau_2; x_0, \tau_0)} dx_0 dx_2. \quad (15)$$

In Figure 8 (top panel) we report the power spectral density (PSD) of the SME time series (black) along with the PSD of the time series obtained through the model (red). The comparison shows that unlike the SME index, the PSD associated with the model outcome exhibits the unique spectral trend  $f^{-2}$ . A comparison of the  $D_{KL}(p_E||p_{CK})$  between SME (blue) and the model (red) as a function of the time scale is reported in the bottom panel. In the case of the SDE, we report the values of the KL divergence averaged over 20 realizations along with the  $\pm 3\sigma$  level (shaded area). We observe that the SME index can be described as a Markov process at small scales. Around  $\tau \sim 60$  min (vertical dashed line) the KL divergence associated with



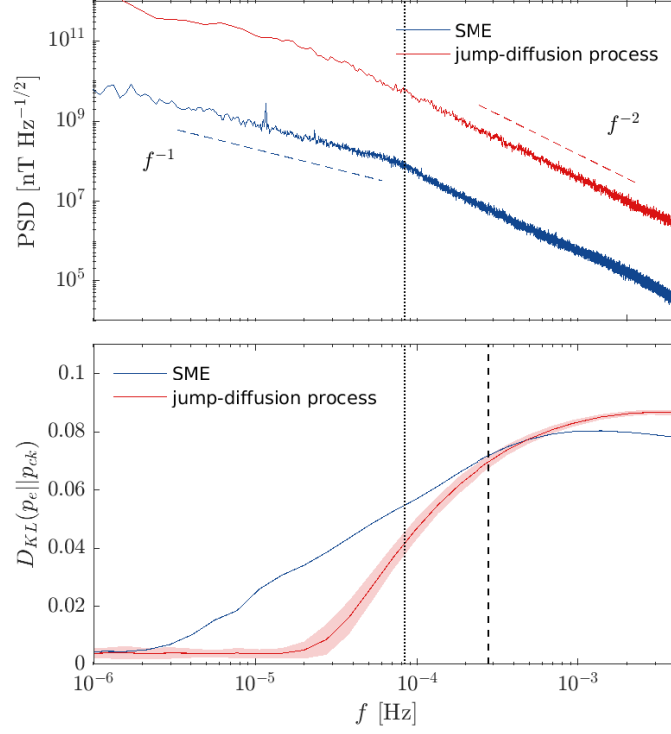


Figure 8: Top panel: Power spectral density of the SME index (blue) and of the SDE model (red). The  $f^{-1}$  and  $f^{-2}$  trends are reported as a guide for the eye. The vertical dotted line indicates the spectral break of the SME index. Bottom panel: KL divergence of  $p_E$  and  $p_{CK}$  for the SME index (blue) and the SDE model (red). In the case of the SDE model the curve is averaged over 50 independent realizations of the process. The red shaded area represents the  $\pm 3\sigma$  bounds and the vertical red line indicates the frequency (corresponding to  $\sim 60$  min) at which the KL divergence of SME overcome the  $3\sigma$  level of the model.

the SME index overcome the  $3\sigma$  threshold of the  $D_{KL}(p_E||p_{CK})$  associated with the model and at time scales above the spectral break, i.e.  $\gtrsim 200$  min, the deviation between the two curves becomes more pronounced. This result points out how the stochastic model can accurately capture the burst-like behavior of the magnetospheric dynamics, but also provides a quantitative information about the violation of the Markov property as a function of  $\tau$ . It is evident that for  $\tau > 60$  min, a deviation between the SME index statistics and the statistics expected for a Markov process starts. For increasing values of  $\tau$  this discrepancy becomes more important suggesting that for a broad interval of scales, i.e. from 60 min up to  $\sim 10^4$  min, long-time correlations become important and the Markov property is no longer satisfied by the magnetospheric activity. This fact is well-known and thus supported by the emergence of a  $f^{-1}$  spectral regime. In this analysis we provide a complete characterization of the transition from Markovian to non-Markovian dynamics across a broad range of time scales in terms of the transition probabilities of the process. We would like to stress the importance of a global stochastic process approach in unveiling some of the key properties of the complex magnetospheric dynamics.

## 5. Discussions and conclusions

The high-latitude magnetospheric dynamics exhibits a very complex behavior. In this work we show that is possible to disentangle the deterministic and stochastic parts constituting the overall SME and SML index dynamics by applying a data analysis technique based on Markov process theory. The results confirm that the magnetospheric dynamics can be described as a Markov process at short timescales (i.e.  $\lesssim 60$  min) and that both SME and SML index dynamics present a burst-like activity that produces non-vanishing high-order KM coefficients. These coefficients show an increasing trend as a function of the index values and we showed that their contribution to the overall dynamics can be interpreted in terms of a Poisson-like jump process. We provide evidence that the simple framework of the jump process with Gaussian distributed amplitudes is quite accurate and capture many features of the SME dynamics, especially in reproducing the burst-like magnetospheric activity mainly associated with the occurrence of substorms. This jump dynamics is quite well consistent with the idea that the Earth's magnetospheric response during substorms as monitored by AE indices could resemble a fractional truncated Lévy motion [15]. Furthermore,

the jump dynamics has to be related to the occurrence of impulsive energy releases in the CPS region due to dynamical transitions in a complex fitness space [33, 34]. On the other hand, the Markov character of the dynamics of these indices at timescales shorter than 200 min could be the counterpart of the random superposition of sporadic intermittent reconnection and plasma energization/acceleration phenomena occurring in the geomagnetic CPS near-Earth region as observed in several works [35, 36, 27]. These sporadic events of energy relaxation appear as a random sequence of bursts in the AE index that can also partially superimpose one to the other without any characteristic timescale. As a consequence of these random temporal distribution of single activity bursts a  $\sim 1/f^2$  interval can be observed in the power spectral density of these indices. This point of view is supported by simple numerical simulations [37, 26].

An interesting result of our analysis is that we can associate the different terms (i.e., drift, diffusion and jump parameters) to different physical mechanisms. The SML dynamics, mainly related to the geomagnetic tail, contributes mostly in the burst-like behavior and can be represented as a stochastic process. Conversely, the global convective processes in the magnetosphere, mainly represented by the SMU index, result in a more deterministic contribution to the SME dynamics.

As a last step, we stress that the SDE enabling us to accurately model the SME dynamics, provides also a threshold for the Markov property of the real SME index. This is calculated as the KL divergence between the observed  $p_E$  and the transition probability expected from the CK equation,  $p_{CK}$ . We find that the  $3\sigma$  level with respect to the Markov condition are exceeded around 60 min. Hence, for timescales  $\gtrsim 60$  min, the history of the SME index starts to influence the dynamics in a non-trivial way and consequently the deviation from the Markov property increases as a function of  $\tau$ . Thus, there is a broad interval of scales where the magnetospheric dynamics cannot be reproduced by assuming a simple “memoryless” process. At this long timescales the dynamics of the magnetosphere as monitored by SME displays a power spectral density characterized by a  $1/f$  region which is the counterpart of a long-time correlated dynamics. The emergence of this  $1/f$  domain, as already discussed in several past works [27, 34] could be the evidence for an overlapping/interaction between single substorm bursts [37].

Our results present fundamental implication in the field of Space Weather since our approach, based on data analysis in a stochastic process perspective, is able to unveil some of the key properties of the complex magneto-

spheric activity in response to solar wind changes. Indeed, as also reported in a recent work using a stochastic approach [38], the overall dynamics of the magnetosphere, as represented by the low-latitude geomagnetic index SYM-H, consists of meta-stable states that are mainly driven and connected to the solar wind and interplanetary medium variability. By looking at the scale-dependence of the nature of these states Alberti et al. [38] noted that the slow dynamics, occurring at scales larger than 200 min, is the main responsible of the observed meta-stability of the magnetospheric dynamics; conversely, the fast dynamics ( $\tau \lesssim 100 - 200$  min) mainly persists in its stable state characterized by an increased level of stochasticity during geomagnetic storms, mainly related to the internal dynamics of the magnetosphere [39]. Our results thus suggest that similar findings can be also observed for the high-latitude activity where a clear separation between directly-driven processes and loading/unloading mechanisms are present. The observed scale-separation highlighted in the present study in terms of the Markov property can be related to the different origin of processes involved into the overall dynamics of the SME/SML indices. While the "memoryless" character of the fast dynamics is mainly related to the occurrence of internal dynamical processes, only triggered by the solar activity, the increased time correlation nature at long timescales is the reflection of the driving effects of the surrounding solar wind. Thus, a proper modeling of the high-latitude variability must consider both drift and diffusion-jump processes to reproduce the burst-like component due to the geomagnetic tail activity and the forcing effects from the external solar wind. However, being the geospace environment a complex system, its components can react differently to the external forcing from the solar wind, thus producing different effects, both in terms of amplitude and occurrence, at both high and low latitudes. Our approach can be helpful to provide a simple model able to reproduce the statistical features of the high-latitude activity and can be used to provide thresholds in terms of auroral activity that can be used for Space Weather purposes.

The results presented in this paper rely on data collected at SuperMAG.

We gratefully acknowledge the SuperMAG collaborators (<http://supermag.jhuapl.edu/info/?pa>

S.B. and G.C. acknowledge the financial support by Italian MIUR-PRIN grant 2017APKP7T on Circumterrestrial Environment: Impact of Sun-Earth Interaction. M.S. acknowledges the National Institute for Astrophysics, the University of Rome "Tor Vergata" and the University of Rome "La Sapienza" for the joint Ph.D. program "Astronomy, Astrophysics and Space Science".

G.C. and T.A. acknowledge fruitful discussions within the scope of the International Team “Complex Systems Perspectives Pertaining to the Research of the Near-Earth Electromagnetic Environment” at the International Space Science Institute in Bern, Switzerland.

## References

- [1] B. T. Tsurutani, M. Sugiura, T. Iyemori, B. E. Goldstein, W. D. Gonzalez, S. I. Akasofu, E. J. Smith, The nonlinear response of AE to the IMF  $B_S$  driver: A spectral break at 5 hours, *Geophysical Research Letters* 17 (3) (1990) 279–282. doi:10.1029/GL017i003p00279.
- [2] D. N. Baker, A. J. Klimas, R. L. McPherron, J. Buechner, The evolution from weak to strong geomagnetic activity: An interpretation in terms of deterministic chaos, *Geophysical Research Letters* 17 (1) (1990) 41–44. doi:10.1029/GL017i001p00041.
- [3] A. J. Klimas, D. Vassiliadis, D. N. Baker, D. A. Roberts, The organized nonlinear dynamics of the magnetosphere, *Journal of Geophysical Research (Space Physics)* 101 (A6) (1996) 13089–13114. doi:10.1029/96JA00563.
- [4] G. Consolini, M. F. Marcucci, M. Candidi, Multifractal Structure of Auroral Electrojet Index Data, *Physical Review Letters* 76 (21) (1996) 4082–4085. doi:10.1103/PhysRevLett.76.4082.
- [5] G. Consolini, T. S. Chang, Magnetic Field Topology and Criticality in Geotail Dynamics: Relevance to Substorm Phenomena, *Space Science Reviews* 95 (2001) 309–321. doi:10.1023/A:1005252807049.
- [6] V. M. Uritsky, A. J. Klimas, D. Vassiliadis, D. Chua, G. Parks, Scale-free statistics of spatiotemporal auroral emissions as depicted by POLAR UVI images: Dynamic magnetosphere is an avalanching system, *Journal of Geophysical Research (Space Physics)* 107 (A12) (2002) 1426. doi:10.1029/2001JA000281.
- [7] T. Chang, S. W. Y. Tam, C.-C. Wu, G. Consolini, Complexity, Forced and/or Self-Organized Criticality, and Topological Phase Transitions in Space Plasmas, *Space Science Reviews* 107 (1) (2003) 425–445. doi:10.1023/A:1025502023494.

- [8] Y. Kamide, The importance of the variability of the solar-terrestrial environment, Washington DC American Geophysical Union Geophysical Monograph Series 60 (1990) 23–23. doi:10.1029/GM060p0023.
- [9] W. D. Gonzalez, A. L. Clúa de Gonzalez, B. T. Tsurutani, Geomagnetic response to large-amplitude interplanetary Alfvén wave trains, *Physica Scripta* Volume T 55 (1994) 140.
- [10] J. G. Lyon, The Solar Wind-Magnetosphere-Ionosphere System, *Science* 288 (5473) (2000) 1987–1991. doi:10.1126/science.288.5473.1987.
- [11] J. E. Borovsky, J. A. Valdivia, The Earth’s Magnetosphere: A Systems Science Overview and Assessment, *Surveys in Geophysics* 39 (5) (2018) 817–859. doi:10.1007/s10712-018-9487-x.
- [12] T. N. Davis, M. Sugiura, Auroral electrojet activity index AE and its universal time variations, *Journal of Geophysical Research* 71 (3) (1966) 785–801. doi:10.1029/JZ071i003p00785.
- [13] T. Iyemori, Storm-time magnetospheric currents inferred from mid-latitude geomagnetic field variations, *Journal of Geomagnetism and Geoelectricity* 42 (11) (1990) 1249–1265. doi:10.5636/jgg.42.1249.
- [14] J. Gjerloev, The supermag data processing technique, *Journal of Geophysical Research: Space Physics* 117 (A9) (2012).
- [15] N. W. Watkins, D. Credington, B. Hnat, S. C. Chapman, M. P. Freeman, J. Greenhough, Towards Synthesis of Solar Wind and Geomagnetic Scaling Exponents: A Fractional Lévy Motion Model, *Space Science Reviews* 121 (1-4) (2005) 271–284. arXiv:physics/0509058, doi:10.1007/s11214-006-4578-2.
- [16] G. Consolini, M. Kretzschmar, A. T. Lui, G. Zimbardo, W. M. Macek, On the magnetic field fluctuations during magnetospheric tail current disruption: A statistical approach, *Journal of Geophysical Research: Space Physics* 110 (A7) (2005).
- [17] A. Pulkkinen, A. Klimas, D. Vassiliadis, V. Uritsky, Role of stochastic fluctuations in the magnetosphere-ionosphere system: A stochastic model for the ae index variations, *Journal of Geophysical Research: Space Physics* 111 (A10) (2006).

- [18] M. Rypdal, K. Rypdal, Stochastic modeling of the ae index and its relation to fluctuations in bz of the imf on time scales shorter than substorm duration, *Journal of Geophysical Research: Space Physics* 115 (A11) (2010).
- [19] T. Chang, Self-organized criticality, multi-fractal spectra, and intermittent merging of coherent structures in the magnetotail, *Astrophysics and space science* 264 (1) (1998) 303–316.
- [20] G. Consolini, T. Chang, A. T. Lui, Complexity and topological disorder in the earth’s magnetotail dynamics, in: *Nonequilibrium Phenomena in Plasmas*, Springer, 2005, pp. 51–69.
- [21] R. Friedrich, J. Peinke, M. Sahimi, M. R. R. Tabar, Approaching complexity by stochastic methods: From biological systems to turbulence, *Physics Reports* 506 (5) (2011) 87–162.
- [22] P. Newell, J. Gjerloev, Evaluation of supermag auroral electrojet indices as indicators of substorms and auroral power, *Journal of Geophysical Research: Space Physics* 116 (A12) (2011).
- [23] Y. Kamide, S. Kokubun, Two-component auroral electrojet: Importance for substorm studies, *Journal of Geophysical Research* 101 (A6) (1996) 13027–13046. doi:10.1029/96JA00142.
- [24] G. Consolini, P. De Michelis, Local intermittency measure analysis of AE index: The directly driven and unloading component, *Geophysical Research Letters* 32 (5) (2005) L05101. doi:10.1029/2004GL022063.
- [25] P. Newell, J. Gjerloev, Substorm and magnetosphere characteristic scales inferred from the supermag auroral electrojet indices, *Journal of Geophysical Research: Space Physics* 116 (A12) (2011).
- [26] A. J. Klimas, J. A. Valdivia, D. Vassiliadis, D. N. Baker, M. Hesse, J. Takalo, Self-organized criticality in the substorm phenomenon and its relation to localized reconnection in the magnetospheric plasma sheet, *Journal Geophysical Research* 105 (A8) (2000) 18,765–18,780. doi:10.1029/1999JA000319.

- [27] G. Consolini, Self-organized criticality: A new paradigm for the magnetotail dynamics, *Fractals* 10 (03) (2002) 275–283. doi:10.1142/S0218348X02001397.
- [28] H. Risken, Fokker-planck equation, in: *The Fokker-Planck Equation*, Springer, 1996, pp. 63–95.
- [29] K. Lehnertz, L. Zabawa, M. R. Rahimi Tabar, Characterizing abrupt transitions in stochastic dynamics, *New Journal of Physics* 20 (11) (2018) 113043. doi:10.1088/1367-2630/aaf0d7.
- [30] M. Anvari, M. R. R. Tabar, J. Peinke, K. Lehnertz, Disentangling the stochastic behavior of complex time series, *Scientific Reports* 6 (2016) 35435. doi:10.1038/srep35435.
- [31] N. Bruti-Liberati, E. Platen, Approximation of jump diffusions in finance and economics, *Computational Economics* 29 (3) (2007) 283–312.
- [32] B. Tsurutani, R. Hajra, E. Echer, J. Gjerloev, Extremely intense ( $sml \leq -2500$  nt) substorms: isolated events that are externally triggered?, in: *Annales Geophysicae*, Vol. 33, Copernicus GmbH, 2015, pp. 519–524.
- [33] A. S. Sharma, M. I. Sitnov, K. Papadopoulos, Substorms as nonequilibrium transitions of the magnetosphere, *Journal of Atmospheric and Solar-Terrestrial Physics* 63 (13) (2001) 1399–1406. doi:10.1016/S1364-6826(00)00241-8.
- [34] G. Consolini, P. de Michelis, Fractal time statistics of AE-index burst waiting times: evidence of metastability, *Nonlinear Processes in Geophysics* 9 (2002) 419–423. doi:10.5194/npg-9-419-2002.
- [35] A. T. Y. Lui, K. Liou, P. T. Newell, C. I. Meng, S. I. Ohtani, T. Ogino, S. Kokubun, M. J. Brittnacher, G. K. Parks, Plasma and magnetic flux transport associated with auroral breakups, *Geophysical Research Letters* 25 (21) (1998) 4059–4062. doi:10.1029/1998GL900022.
- [36] V. Angelopoulos, T. Mukai, S. Kokubun, Evidence for intermittency in Earth’s plasma sheet and implications for self-organized criticality, *Physics of Plasmas* 6 (11) (1999) 4161–4168. doi:10.1063/1.873681.



- [37] T. Hwa, M. Kardar, Avalanches, hydrodynamics, and discharge events in models of sandpiles, *Physical Review A* 45 (10) (1992) 7002–7023. doi:10.1103/PhysRevA.45.7002.
- [38] T. Alberti, G. Consolini, P. De Michelis, M. Laurenza, M. F. Marcucci, On fast and slow Earth’s magnetospheric dynamics during geomagnetic storms: a stochastic Langevin approach, *Journal of Space Weather and Space Climate* 8 (2018) A56. doi:10.1051/swsc/2018039.
- [39] T. Alberti, G. Consolini, F. Lepreti, M. Laurenza, A. Vecchio, V. Carbone, Timescale separation in the solar wind-magnetosphere coupling during St. Patrick’s Day storms in 2013 and 2015, *Journal of Geophysical Research (Space Physics)* 122 (4) (2017) 4266–4283. doi:10.1002/2016JA023175.